www.nature.com/cdd

CDDpress

ARTICLE

Apoptotic caspase-7 activation inhibits non-canonical pyroptosis by GSDMB cleavage

Xu Li[1,2,4], Tianxun Zhang[1,4], Lulu Kang[1], Ruyue Xin[1], Minli Sun[1], Qianyue Chen[1], Jingwen Pei[1], Qin Chen[3], Xiang Gao[1]✉ and Zhaoyu Lin[1]✉

© The Author(s), under exclusive licence to ADMC Associazione Differenziamento e Morte Cellulare 2023

GSDMB is associated with several inflammatory diseases, such as asthma, sepsis and colitis. GZMA is released by cytotoxic lymphocytes and cleaves GSDMB at the K244 site and to induce GSDMB N-terminus dependent pyroptosis. This cleavage of GSDMB is noncell autonomous. In this study, we demonstrated that the GSDMB-N domain (1-91 aa) was important for a novel cell-autonomous function and that GSDMB could bind caspase-4 and promote noncanonical pyroptosis. Furthermore, activated caspase-7 cleaved GSDMB at the D91 site to block GSDMB-mediated promotion of noncanonical pyroptosis during apoptosis. Mechanistically, the cleaved GSDMB-C-terminus (92-417 aa) binds to the GSDMB-N-terminus (1-91 aa) to block the function of GSDMB. During *E. coli* and *S. Typhimurium* infection, inhibition of the caspase-7/GSDMB axis resulted in more pyroptotic cells. Furthermore, in a septic mouse model, caspase-7 inhibition or deficiency in GSDMB-transgenic mice led to more severe disease phenotypes. Overall, we demonstrate that apoptotic caspase-7 activation inhibits non-canonical pyroptosis by cleaving GSDMB and provide new targets for sepsis therapy.

Cell Death & Differentiation (2023) 30:2120–2134; https://doi.org/10.1038/s41418-023-01211-3

INTRODUCTION

GSDMB is a gasdermin family member. GSDMB is considered an oncogene and is correlated with worse outcomes in several cancers [1–3]. Furthermore, *GSDMB* is related to the susceptibility of inflammatory diseases, such as sepsis, asthma and inflammatory bowel disease [4–6]. Until now, the physiological function of GSDMB has remained unclear.

Existing studies have demonstrated that the majority of gasdermin family members, including GSDMB, can act as pyroptotic executors. Granzyme A cleaves GSDMB at the K244 site and induces toxic N-terminus (1-244 aa)-mediated pyroptosis. This pathway plays an important role in antitumor immunity and intracellular bacterial killing [7, 8]. During this process, the cleavage of GSDMB is noncell-autonomous and is dependent on granzyme A released by neighboring cytotoxic lymphocytes. Our previous work demonstrated that GSDMB enhanced caspase-4 enzyme activity to promote noncanonical pyroptosis, suggesting that GSDMB has cell-autonomous functions [6].

Noncanonical pyroptosis is rapid inflammatory cell death and can induce the quick release of inflammatory factors. It is associated with a more severe disease phenotype in sepsis. *Caspase-11*$^{-/-}$ septic mice showed impaired noncanonical pyroptosis and a significantly increased survival rate [9, 10]. Nedd4 (an E3 ubiquitin ligase) deficiency and sphingosine-1-phosphate receptor 2 activation promote noncanonical pyroptosis and exacerbate sepsis [11, 12]. In contrast, apoptosis is a relatively mild noninflammatory cell death. The balance between apoptosis and noncanonical pyroptosis is important in inflammatory diseases. Caspase-3/7 are important executors of apoptosis [13]. Furthermore, activated caspase-3/7 can cleave GSDMB [6, 14]. This finding indicates that the caspase-3, 7/GSDMB axis may play a role in the balance between apoptosis and noncanonical pyroptosis.

In this study, we found that activated apoptotic caspase-7, but not caspase-3 inhibited noncanonical pyroptosis by cleaving GSDMB. Furthermore, inhibition or deficiency of caspase-7 in GSDMB-transgenic mice leads to more severe sepsis phenotypes, suggesting that caspase-7-related apoptotic inhibition of non-canonical pyroptosis is the self-protective pathway for the host. Furthermore, this pathway might be a potential therapeutic target for sepsis in the future.

RESULTS

GSDMB is cleaved during apoptosis

Consistent with previous reports [6, 14], we found that the overexpression of activated caspase-3/7 cleaved GSDMB in HEK293T cells (Fig. 1A). Since caspase-3 and caspase-7 are activated during apoptosis [13], we explored whether GSDMB could be cleaved during apoptosis. Staurosporine (STAU) and cycloheximide (CHX) are typical apoptotic activators (Fig. 1H) [15–20]. Our data showed that significant cleavage of GSDMB was detected in 3xflag-GSDMB overexpressing HeLa cells during

[1]State Key Laboratory of Pharmaceutical Biotechnology, MOE Key Laboratory of Model Animals for Disease Study, Jiangsu Key Laboratory of Molecular Medicine, Model Animal Research Center, National Resource Center for Mutant Mice of China, Nanjing Drum Tower Hospital, School of Medicine, Nanjing University, Nanjing 210061, China. [2]Institutes for Systems Genetics, Frontiers Science Center for Disease-related Molecular Network, National Clinical Research Center for Geriatrics, West China Hospital, Sichuan University, Chengdu, China. [3]Department of Oral Surgery, Shanghai Jiao Tong University, 639 Zhizaoju Road, Huangpu District, Shanghai, CN 200240, China. [4]These authors contributed equally: Xu Li, Tianxun Zhang. ✉email: gaoxiang@nju.edu.cn; linzy@nju.edu.cn

Received: 22 August 2022 Revised: 3 August 2023 Accepted: 9 August 2023
Published online: 17 August 2023

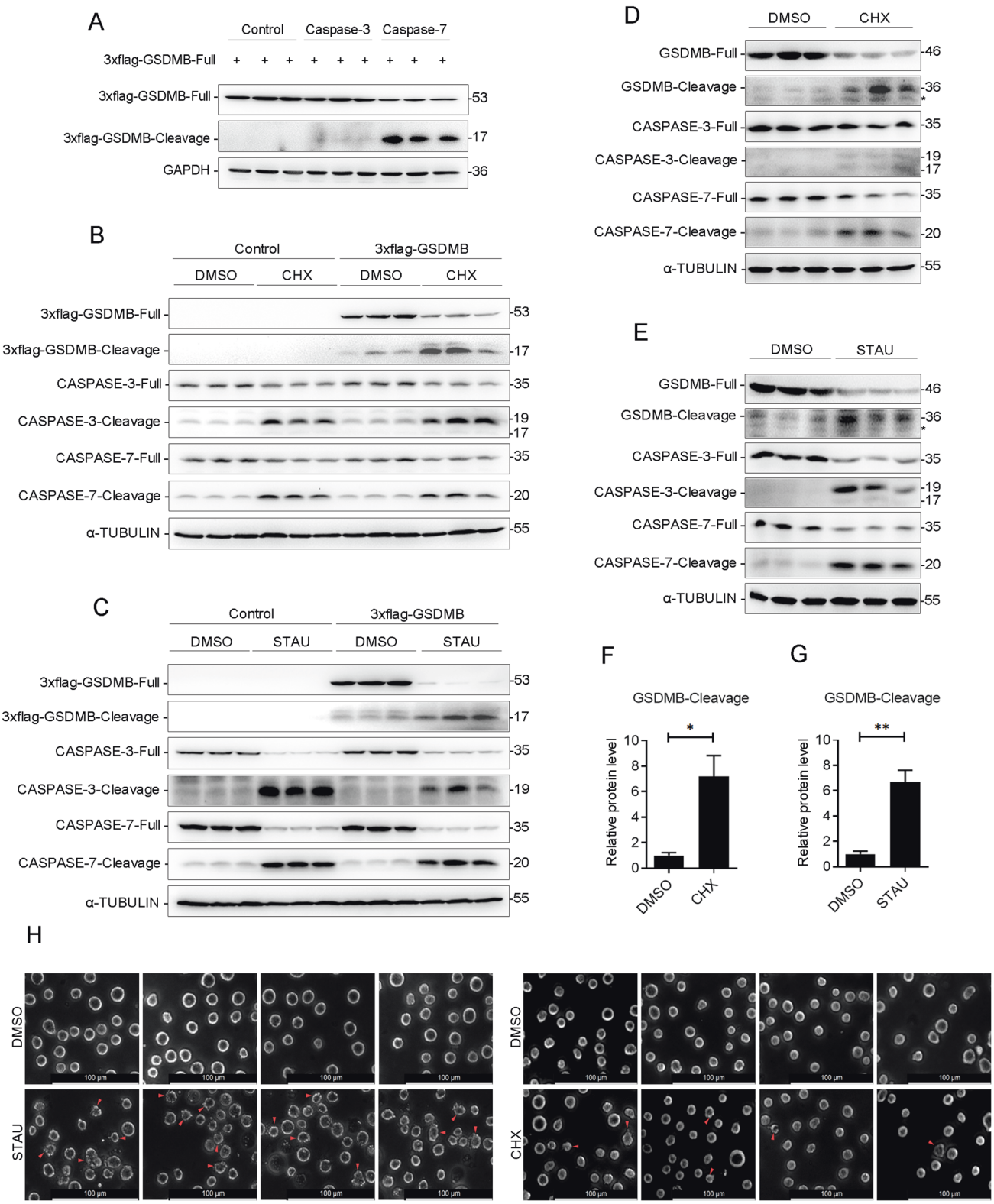

apoptosis induced by CHX or STAU (Fig. 1B, C). Consistently, cleavage of endogenous GSDMB was observed in apoptotic THP-1 cells treated with CHX or STAU (Fig. 1D–G). Since STAU could induce more severe apoptosis in THP-1 cells than CHX, it was used as a proapoptotic reagent in subsequent experiments (Fig. 1H). These results suggest that GSDMB is cleaved during the physiological process of apoptosis.

Apoptosis inhibits noncanonical pyroptosis

Full-length GSDMB significantly promotes noncanonical pyroptosis [6]. Our results showed that GSDMB could be cleaved during apoptosis (Fig. 1). It would be interesting to check whether the activation of apoptosis could inhibit noncanonical pyroptosis promoted by GSDMB. We induced apoptosis with STAU and noncanonical pyroptosis with LPS electroporation in THP-1 cells.

Fig. 1 GSDMB is cleaved during apoptosis. A Immunoblotting for 3xflag-GSDMB-Full and 3xflag-GSDMB-Cleavage in whole cell lysates of HEK293T cells overexpressing the 3xflag-GSDMB-Full and activated CASPASE-3 (p12 and p17) or activated CASPASE-7 (p11 and p20). GAPDH is used as a loading control. **B** Immunoblotting for 3xflag-GSDMB-Full, 3xflag-GSDMB-Cleavage, CASPASE-3-Full, CASPASE-7-Full, CASPASE-3-Cleavage and CASPASE-7-Cleavage in whole cell lysates of indicated HeLa cells. α-TUBULIN is used as a loading control. HeLa cells transfected with 3xflag-GSDMB and control plasmids were treated with 80uM CHX for 3.5 h (DMSO as control). **C** Immunoblotting for 3xflag-GSDMB-Full, 3xflag-GSDMB-Cleavage, CASPASE-3-Full, CASPASE-7-Full, CASPASE-3-Cleavage and CASPASE-7-Cleavage in whole cell lysates of indicated HeLa cells. α-TUBULIN is used as a loading control. HeLa cells transfected with 3xflag-GSDMB and control plasmids were treated with 8uM STAU (DMSO as control) for 3.5 h. **D** Immunoblotting for GSDMB-Full, GSDMB-Cleavage, CASPASE-3-Full, CASPASE-3-Cleavage, CASPASE-7-Full and CASPASE-7-Cleavage in whole cell lysates of indicated THP-1 cells. α-TUBULIN is used as a loading control. THP-1 cells were treated with 50 uM CHX for 4 h (DMSO as control). Non-specific bands are indicated with an asterisk (*). **E** Immunoblotting for GSDMB-Full, GSDMB-Cleavage, CASPASE-3-Full, CASPASE-3-Cleavage, CASPASE-7-Full and CASPASE-7-Cleavage in whole cell lysates of indicated THP-1 cells. α-TUBULIN is used as a loading control. THP-1 cells were treated with 1.34 uM STAU for 2.5 h (DMSO as control). Non-specific bands are indicated with an asterisk (*). **F** The gray scale analysis of GSDMB-Cleavage/GSDMB-Full in (**D**). **G** The gray scale analysis of GSDMB-Cleavage/GSDMB-Full in (**E**). **H** Representative brightfield cell images. Representative apoptotic THP-1 cells are indicated with red arrows. Bar = 100 μm. **F**, **G** Each panel is a representative experiment of at least three replicates. Data are presented as the mean ± SD. *T*-test: $*p < 0.05$, $**p < 0.01$. Full = full length. All the 3xflag-tagged proteins were detected with anti-flag antibodies. Endogenous GSDMB proteins were detected with anti-GSDMB antibodies.

First, we examined the efficiency of LPS electroporation by LPS-FITC analysis. We confirmed that apoptotic and nonapoptotic cells were equally able to take up LPS (Supplementary Fig. 1A). GSDMD cleavage and LDH release in the apoptosis+pyroptosis (STAU + LPS) group were significantly downregulated compared with those in pyroptosis (DMSO + LPS) group (Fig. 2A, B, D). Moreover, the cleavage of GSDMB was significantly increased in the apoptosis (STAU) and apoptosis+pyroptosis (STAU + LPS) groups compared to the control groups (Fig. 2A, C). We performed Annexin V-FITC and PI staining to detect cell death by FACS (Fig. 2E, G and Supplementary Fig. 1E), as previously reported [21]. The apoptotic cells in late stage and the pyroptotic cells are supposed to be Annexin V/PI double positive. To compare the percentage of pyroptotic cells in pyroptosis (DMSO + LPS) group and apoptosis + pyroptosis (STAU + LPS) group, we analyzed the relative pyroptotic cells. We screened effective siRNAs targeting *CASPASE-4* and *CASPASE-5* as the negative control (Supplementary Fig. 1B–D). Compared to the pyroptosis (DMSO + LPS) group, the percentage of relative pyroptotic cells was significantly decreased in the apoptosis+pyroptosis (STAU + LPS) group in WT THP-1 cells, while there were no relative pyroptotic cells in *CASPASE4/5*-knockdown THP-1 cells (Fig. 2E, G). Consistently, the percentages of live cells were significantly decreased only in the pyroptosis (DMSO + LPS) group and apoptosis+pyroptosis (STAU + LPS) group of WT THP-1 cells, but not in *CASPASE4/5*-knockdown cells (Fig. 2F, G), which suggested that LPS-induced cell death is mainly CASPASE-4/5-mediated noncanonical pyroptosis. In summary, these results suggest that apoptosis significantly inhibits non-canonical pyroptosis, which correlated with GSDMB cleavage.

Apoptotic inhibition of noncanonical pyroptosis is dependent on caspase-7

Although activated CASPASE-3 and CASPASE-7 can both cleave GSDMB, the efficiency of CASPASE-7 is much higher (Fig. 1A). Our goal was to explore whether these two caspases play critical roles in apoptotic inhibition of noncanonical pyroptosis. We screened effective siRNAs targeting *CASPASE-3* and *CASPASE-7* for subsequent experiments (Supplementary Figs. 2A, B and 3A, B). After *CASPASE-7* knockdown, GSDMD cleavage and LDH release were not different between the pyroptosis (DMSO + LPS) group and the apoptosis +pyroptosis (STAU + LPS) group, suggesting that apoptosis could not inhibit noncanonical pyroptosis in *CASPASE-7*-knockdown THP-1 cells (Fig. 3A–C and Supplementary Fig. 2C–E). In contrast, the cleavage of GSDMD and LDH release remained significantly down-regulated by apoptosis in *CASPASE-3*-knockdown THP-1 cells (Fig. 3D–F and Supplementary Fig. 3C–E). Taken together, these results suggest that apoptotic inhibition of noncanonical pyroptosis is dependent on caspase-7 but not caspase-3.

Apoptotic caspase-6 and caspase-8 have also been confirmed that they could cleave GSDMB in our previous study [6]. Next, we explored if caspase-6 and caspase-8 are involved in GSDMB-mediated noncanonical pyroptosis activation. We screened effective siRNAs targeting *CASPASE-6* and *CASPASE-8* for subsequent experiments (Supplementary Fig. 4A, B, F, G). The GSDMD cleavage and LDH release remained significantly downregulated by apoptosis in *CASPASE-6*-knockdown THP-1 cells (Supplementary Fig. 4C–E). After *CASPASE-8* knockdown, the GSDMD cleavage was significantly downregulated in the apoptosis+pyroptosis (STAU + LPS) group (Supplementary Fig. 4H, I). However, the LDH release was not different between the pyroptosis (DMSO + LPS) group and the apoptosis+pyroptosis (STAU + LPS) group in *CASPASE-8*-knockdown THP-1 cells (Supplementary Fig. 4J), which might be due to the activation of necroptosis after caspase-8 knockdown [22]. Our data showed that significant phosphorylation of MLKL was detected in caspase-8-knockdown THP-1 cells during apoptosis (Supplementary Fig. 4K). Overall, apoptotic inhibition of noncanonical pyroptosis is independent of caspase-6 and caspase-8.

Caspase-7-mediated GSDMB cleavage is necessary for apoptotic inhibition of noncanonical pyroptosis

Activated caspase-3/7 can cleave GSDMB at the D91 site [20, 21]. Our previous data indicated that the caspase-7/GSDMB axis might play an important role in apoptotic inhibition of noncanonical pyroptosis (Figs. 1–3). To confirm the role of the caspase-7/GSDMB axis, we mutated GSDMB D91 to A91. As expected, directly activated CASPASE-3/7 could not cleave D91A-GSDMB in HEK293T cells (Supplementary Fig. 5A). Furthermore, in apoptotic cells, D91A-GSDMB could not be cleaved (Supplementary Fig. 5B). The cleavage of GSDMD was not inhibited when the cells were cotransfected with D91A-GSDMB in STAU + LPS group (Supplementary Fig. 5C, D). Furthermore, the LDH release results showed no difference between the pyroptosis (DMSO + LPS) group and apoptosis+pyroptosis (STAU + LPS) group when the cells were transfected with D91A-GSDMB (Supplementary Fig. 5E), suggesting that apoptosis could not inhibit noncanonical pyroptosis when D91 was mutated to A91. However, we found that the GSDMD cleavage and LDH release in the pyroptosis (DMSO + LPS) group were significantly downregulated when D91 was mutated to A91. We think it might because the D91 is the key site to mediate full-length GSDMB-related promotion of noncanonical pyroptosis. To exclude the direct effect of D91A mutation, we constructed another GSDMB mutation, D91V. Consistent with D91A-GSDMB, D91V-GSDMB could not be cleaved during STAU-mediated apoptosis (Fig. 4A). D91V-GSDMB did not affect the cleavage of GSDMD without STAU treatment. The GSDMD cleavage and LDH release were not different in pyroptosis (DMSO + LPS) group and apoptosis+pyroptosis (STAU + LPS) group when the cells were cotransfected with D91V-GSDMB, suggesting that apoptosis could not inhibit noncanonical pyroptosis when D91 was mutated to V91 (Fig. 4B–D). In conclusion, caspase-7-mediated

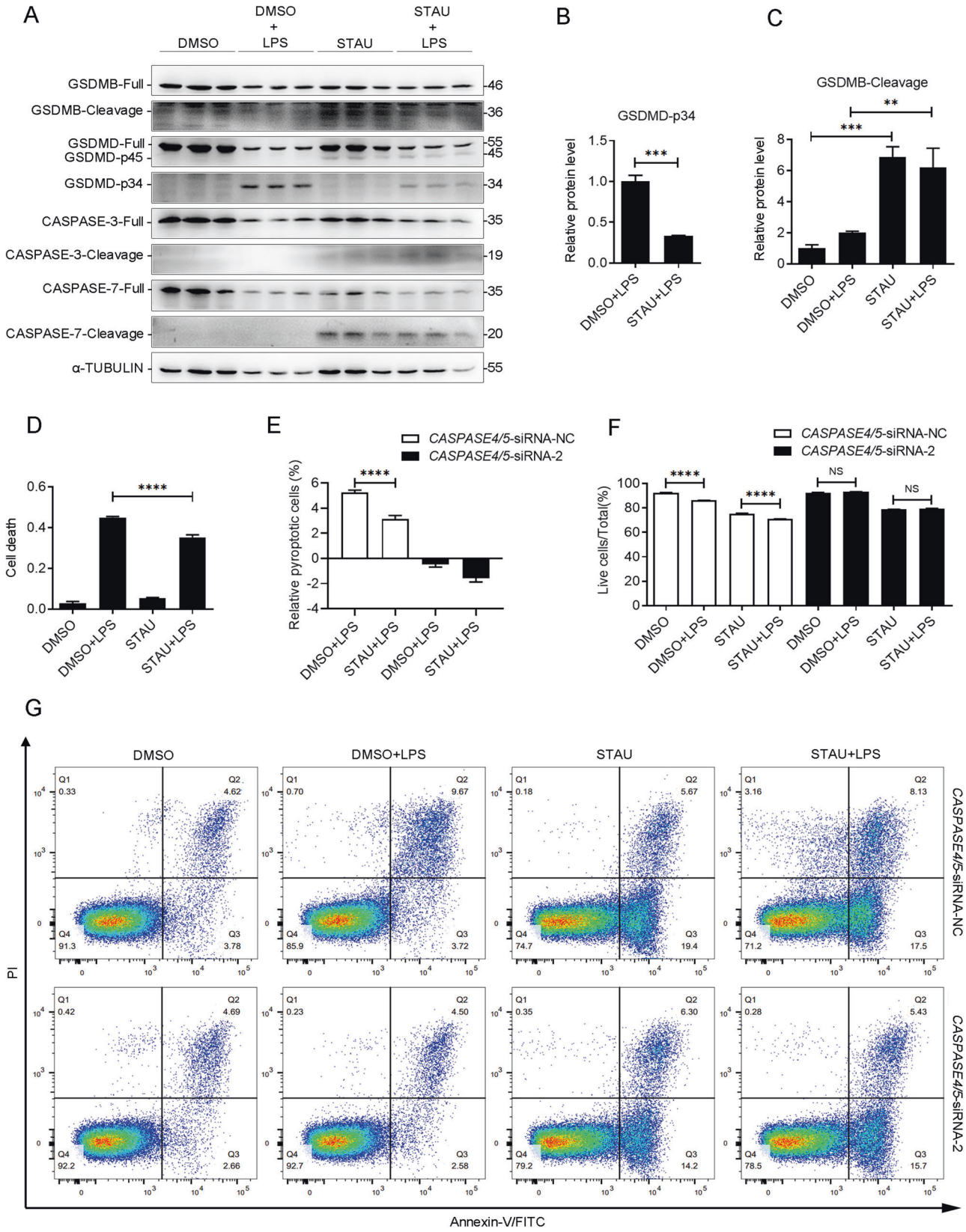

GSDMB cleavage is necessary for the apoptotic inhibition of noncanonical pyroptosis.

Granzyme A produced by cytotoxic immune cells can cleave GSDMB at the K244 site in target cells to produce a pyroptotic N-terminal fragment [7]. Next, we explored whether this pathway affected the balance between apoptosis and noncanonical pyroptosis. As expected, the immunoblot results showed that the K244 site was not cleaved, and its mutation did not affect the

Fig. 2 Apoptosis inhibits non-canonical pyroptosis. A–D THP-1 cells were treated with 1.34 μM STAU (DMSO as control) for 2.5 h and then electrically transferred LPS to induce non-canonical pyroptosis. **A** Immunoblotting for GSDMB-Full, GSDMD-Full, GSDMB-Cleavage, GSDMD-p34, GSDMD-p45, CASPASE-3-Full, CASPASE-7-Full, CASPASE-3-Cleavage and CASPASE-7-Cleavage in whole cell lysates of indicated THP-1 cells. α-TUBULIN is used as a loading control. GSDMD-p34 was generated by D275 cleavage by CASPASE-4. GSDMD-p45 was generated by D87 cleavage by CASPASE-3/7. **B** The gray scale analysis of GSDMD-p34/GSDMD-Full in (**A**). **C** The gray scale analysis of GSDMB-Cleavage/GSDMB-Full in (**A**). **D** LDH assay for cell death in indicated THP-1 cells. **E–G** The cell viability checked by FACS with Annexin V-FITC/PI staining. THP-1 cells were electrically transferred control siRNA (*CASPASE4/5*-siRNA-NC) and *CASPASE4/5* siRNA (*CASPASE4/5*-siRNA-2). After 45 h, the cells were treated with 1.34 μM STAU (DMSO as control) for 2.5 h and then electrically transferred LPS to induce non-canonical pyroptosis. **E** Relative pyroptotic cells in indicated groups. The relative pyroptotic cells of group (DMSO + LPS) = group (DMSO + LPS) - group (DMSO). The relative pyroptotic cells of group (STAU + LPS) = group (STAU + LPS) - group (STAU). **F** Percentage of live cells in indicated groups. **G** Representative flow cytometry plots of indicated THP-1 cells. Q2: pyroptotic cells and late apoptotic cells, Q3: early apoptotic cells, Q4: live cells. Each panel is a representative experiment of at least three replicates. Data are presented as the mean ± SD. **B** *T*-test: ***$p < 0.001$. **C–F** ANOVA followed by Bonferroni's post-test: **$p < 0.01$, ***$p < 0.001$, ****$p < 0.0001$, NS = not significant. Full = full length. Endogenous GSDMB proteins were detected with anti-GSDMB antibodies.

cleavage of GSDMB by CASPASE-7 (Fig. 4E). We further confirmed that apoptosis could significantly inhibit noncanonical pyroptosis when the GSDMB K244 site was mutated to A244 (Fig. 4F, H), suggesting that the granzyme A/GSDMB axis had no effect on cell-autonomous apoptotic inhibition of noncanonical pyroptosis. These results demonstrate that the caspase-7/GSDMB axis and granzyme A/GSDMB axis are different pathways.

Apoptotic inhibition of noncanonical pyroptosis is independent of the caspase-3, -7/GSDMD pathway and caspase-3, -7/GSDME pathway

Activated caspase-3/7 can cleave GSDMD at the D87 site and produce nontoxic N-terminal fragments that fail to induce pyroptosis [23, 24]. Next, we identified whether the caspase-3, -7/GSDMD pathway contributes to the apoptotic inhibition of noncanonical pyroptosis. We confirmed that D87A-GSDMD could not be cleaved by activated CASPASE-3/7 (Supplementary Fig. 6A, B). The cleavage of GSDMD and LDH release data revealed that apoptosis could significantly inhibit noncanonical pyroptosis in the D87A-GSDMD group, demonstrating that the CASPASE-3, -7/GSDMD pathway had no effect on the apoptotic inhibition of noncanonical pyroptosis (Supplementary Fig. 6B–E). This result is consistent with a previous report [25].

GSDME can be cleaved by caspase-3/7 to induce secondary-necroptosis, which is also called apoptotic pyroptosis in cells highly expressing GSDME [26–28]. GSDMB and GSDME can be cleaved by activated CASPASE-7, and both of these pathways are significantly activated when GSDMB and GSDME are over-expressed (Supplementary Fig. 7A). Significant cleavage of GSDME was also detected in apoptotic *CASPASE-3*-knockdown THP-1 cells (Supplementary Fig. 7B). These results indicated that the caspase-7/GSDME pathway might be activated in apoptotic THP-1 cells, which might antagonize the apoptotic inhibition of noncanonical pyroptosis. We screened effective *GSDME* siRNAs for subsequent experiments (Supplementary Fig. 7C, D). The time-course results of LDH release demonstrated that knockdown of GSDME did not affect the activation of pyroptosis during apoptosis, suggesting that the caspase-3, -7/GSDME pathway had no effect on the apoptotic inhibition of noncanonical pyroptosis (Supplementary Fig. 7E).

GSDMB cleaved at the D91 site cannot promote the enzyme activity of caspase-4

Next, we explored the molecular mechanisms underlying the promotion of noncanonical pyroptosis by GSDMB. Full-length GSDMB can bind to caspase-4 to enhance its enzymatic activity [6]. First, we checked the function of the cleaved GSDMB N-terminus (1-91 aa) and C-terminus (92-417 aa) (Fig. 5A). Full-length GSDMB and the N-terminus (1-91 aa) but not the C-terminus (92-417 aa) significantly promoted the cleavage of GSDMD (Fig. 5B). GSDMB-Full could significantly enhance the enzymatic activity of caspase-4, but coexpressed GSDMB N-terminus (1-91 aa) and C-terminus (92-417 aa) could not (Fig. 5C). The Co-IP results showed that the C-terminus (92-417 aa) could significantly inhibit the binding of the N-terminus (1-91 aa) and caspase-4 (Fig. 5D). To identify the key domain of the GSDMB N-terminus (1-91 aa), we induced noncanonical pyroptosis in cells expressing truncated proteins. The results showed that only truncated GSDMB (34-83 aa) lost the ability to promote the cleavage of GSDMD, suggesting that 1-33 aa is the key amino acid sequence that promotes noncanonicalpyroptosis (Fig. 5E).

Additionally, we analyzed the interaction between different fragments of GSDMB (Fig. 5A). As expected, Co-IP experiments validated that the GSDMB C-terminus (92-417 aa) could bind to the N-terminus (1-91 aa) (Fig. 6A). Furthermore, GSDMB (92-244 aa) could bind to GSDMB (1-91 aa), but GSDMB (245-417 aa) could not, suggesting the crucial role of GSDMB (92-244 aa) in the C-terminus (92-417 aa) (Fig. 6B–D). Furthermore, we used fluorescence resonance energy transfer (FRET) to confirm the Co-IP results. There was significant fluorescence colocalization between GSDMB (92-417 aa) and GSDMB (1-91 aa) (Fig. 6F, G). Our data showed that both full-length GSDMB and the GSDMB N-terminus (1-91 aa) promoted pyroptosis (Fig. 5B, C). This finding suggests that the GSDMB C-terminus (92-417 aa) can bind to the GSDMB N-terminus (1-91 aa) to block its function after cleavage at D91.

Previous reports suggested that GSDMB (245-417 aa) binds to GSDMB (1-244aa) before cleavage at K244 [7, 29]. However, our results showed that the GSDMB C-terminus (92-417 aa) only bound to the GSDMB N-terminus (1-91 aa) after cleavage at D91. The reason for the differences between these two binding mechanisms may be that the functional domain of the GSDMB N-terminus (1-91 aa) is 1-33 aa (Fig. 5E) and cannot be blocked by GSDMB (245-417 aa) (Fig. 6C, D). We also found that GSDMB (1-91 aa) and GSDMB (92-244 aa) could not bind to GSDMB (245-417 aa) (Fig. 6C–E), revealing that the reported autoinhibition between GSDMB (1-244 aa) and GSDMB (245-417 aa) is dependent on the amino acid sequence or structure around D91. This finding further indicates that the binding between GSDMB (1-244 aa) and GSDMB (245-417 aa) cannot block the function of GSDMB (1-91 aa) in full-length GSDMB. Furthermore, recent reports on the structural analysis of GSDMB also indicated that the GSDMB-C-terminus (220-411 aa) lacks autoinhibition of the membrane-binding function of the N-terminus (2-226 aa) in full-length GSDMB, revealing a potentially more open structural morphology between the N-terminus and C-terminus of full-length GSDMB [14, 30, 31].

Collectively, we demonstrated that GSDMB could not promote the enzymatic activity of CASPASE-4 when the D91 site was cleaved. The underlying molecular mechanism involves GSDMB (92-417 aa) significantly inhibiting the toxic function of GSDMB (1-91 aa).

Apoptotic inhibition of noncanonical pyroptosis is a self-protective pathway during bacterial infection

Pyroptosis is the rapid inflammatory response to external stimulation, such as bacterial infection. To analyze the

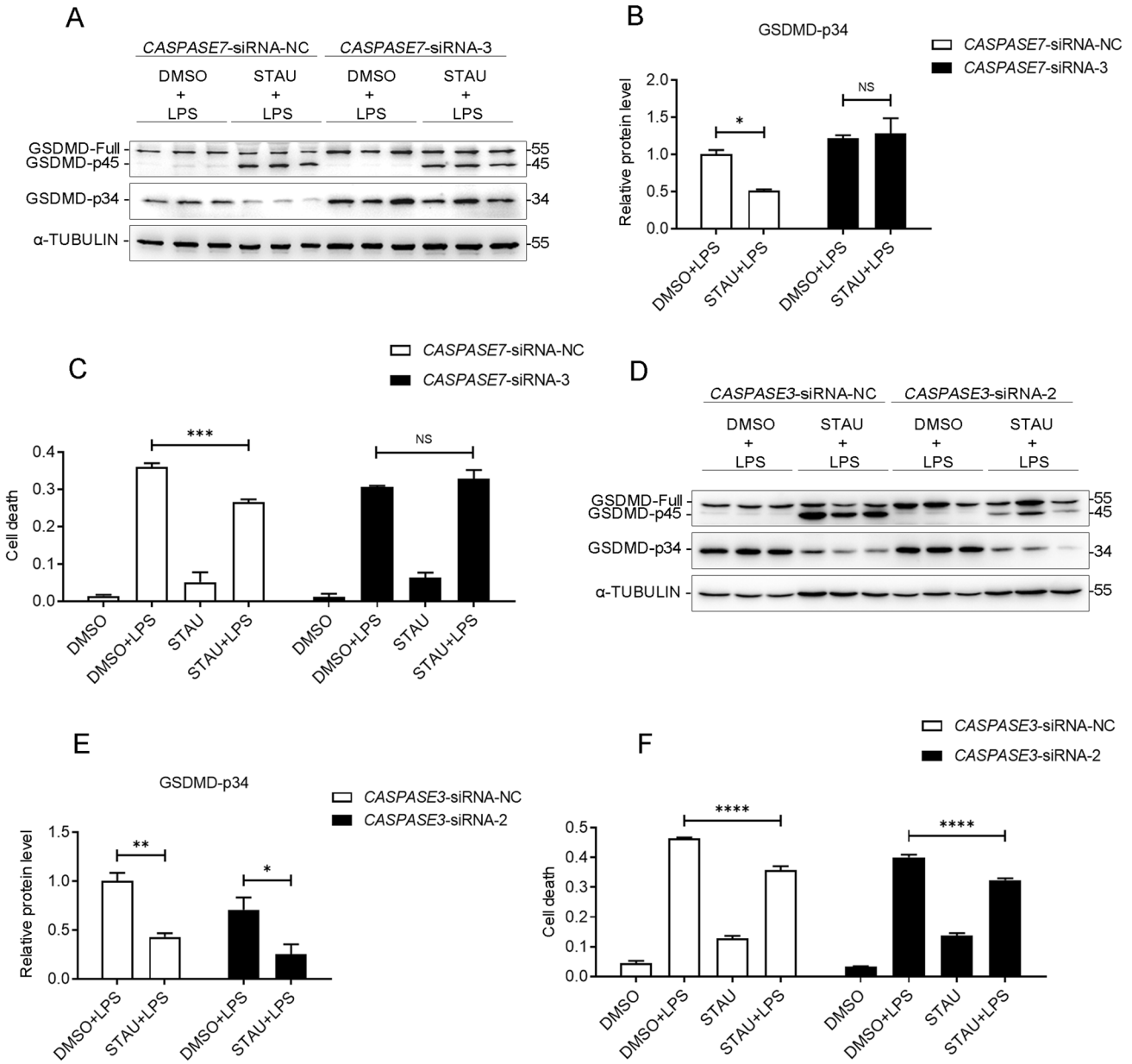

Fig. 3 Apoptotic inhibition of non-canonical pyroptosis is dependent on caspase-7. A–C THP-1 cells were electrically transferred control siRNA (*CASPASE7*-siRNA-NC) and *CASPASE7* siRNA (*CASPASE7*-siRNA-3). After 45 h, the cells were treated with 1.34 μM STAU (DMSO as control) for 2.5 h and then electrically transferred LPS to induce non-canonical pyroptosis. **A** Immunoblotting for GSDMD-Full, GSDMD-p34 and GSDMD-p45 in whole cell lysates of indicated THP-1 cells. α-TUBULIN is used as a loading control. GSDMD-p34 was generated by D275 cleavage by CASPASE-4. GSDMD-p45 was generated by D87 cleavage by CASPASE-3/7. **B** The gray scale analysis of GSDMD-p34/GSDMD-Full in (**A**). **C** LDH assay for cell death in indicated THP-1 cells. **D–F** THP-1 cells were electrically transferred control siRNA (*CASPASE3*-siRNA-NC) and *CASPASE3* siRNA (*CASPASE3*-siRNA-2). After 45 h, the cells were treated with 1.34 μM STAU (DMSO as control) for 2.5 h and then electrically transferred LPS to induce non-canonical pyroptosis. **D** Immunoblotting for GSDMD-Full, GSDMD-p34 and GSDMD-p45 in whole cell lysates of indicated THP-1 cells. α-TUBULIN is used as a loading control. GSDMD-p34 was generated by D275 cleavage by CASPASE-4. GSDMD-p45 was generated by D87 cleavage by CASPASE-3/7. **E** The gray scale analysis of GSDMD-p34/GSDMD-Full in (**D**). **F** LDH assay for cell death in indicated THP-1 cells. Each panel is a representative experiment of at least three replicates. Data are presented as the mean ± SD. **B**, **C**, **E** and **F** ANOVA followed by Bonferroni's post-test: *$p < 0.05$, **$p < 0.01$, ***$p < 0.001$, ****$p < 0.0001$, NS=not significant. Full=full length.

physiological function of the caspase-7/GSDMB pathway during bacterial infection, we used *E. coli* to infect human THP-1 cells. When *CASPASE-7* was knocked down, the secretion of IL-1β significantly increased during *E. coli* infection (Fig. 7A). Correspondingly, knockdown of *CASPASE-7* significantly inhibited the cleavage of GSDMB and promoted the cleavage of GSDMD, suggesting that *CASPASE-7* knockdown enhanced noncanonical pyroptosis during *E. coli* infection (Fig. 7B–D). The live-cell imaging results also showed that more pyroptotic cells were observed during persistent infection with *E. coli* in the *CASPASE-7*-knockdown group than in the control group (Fig. 7E and Supplementary Movie 1). In summary, CASPASE-7-mediated apoptosis inhibits noncanonical pyroptosis during bacterial infection in THP-1 cells.

Since there is no homolog of the human *GSDMB* gene in the mouse genome, to explore the physiological function of GSDMB-related apoptotic inhibition of noncanonical pyroptosis in vivo, we generated BAC-transgenic mice carrying the human *GSDMB* gene and its possible regulatory regions (Supplementary Fig. 8A). We

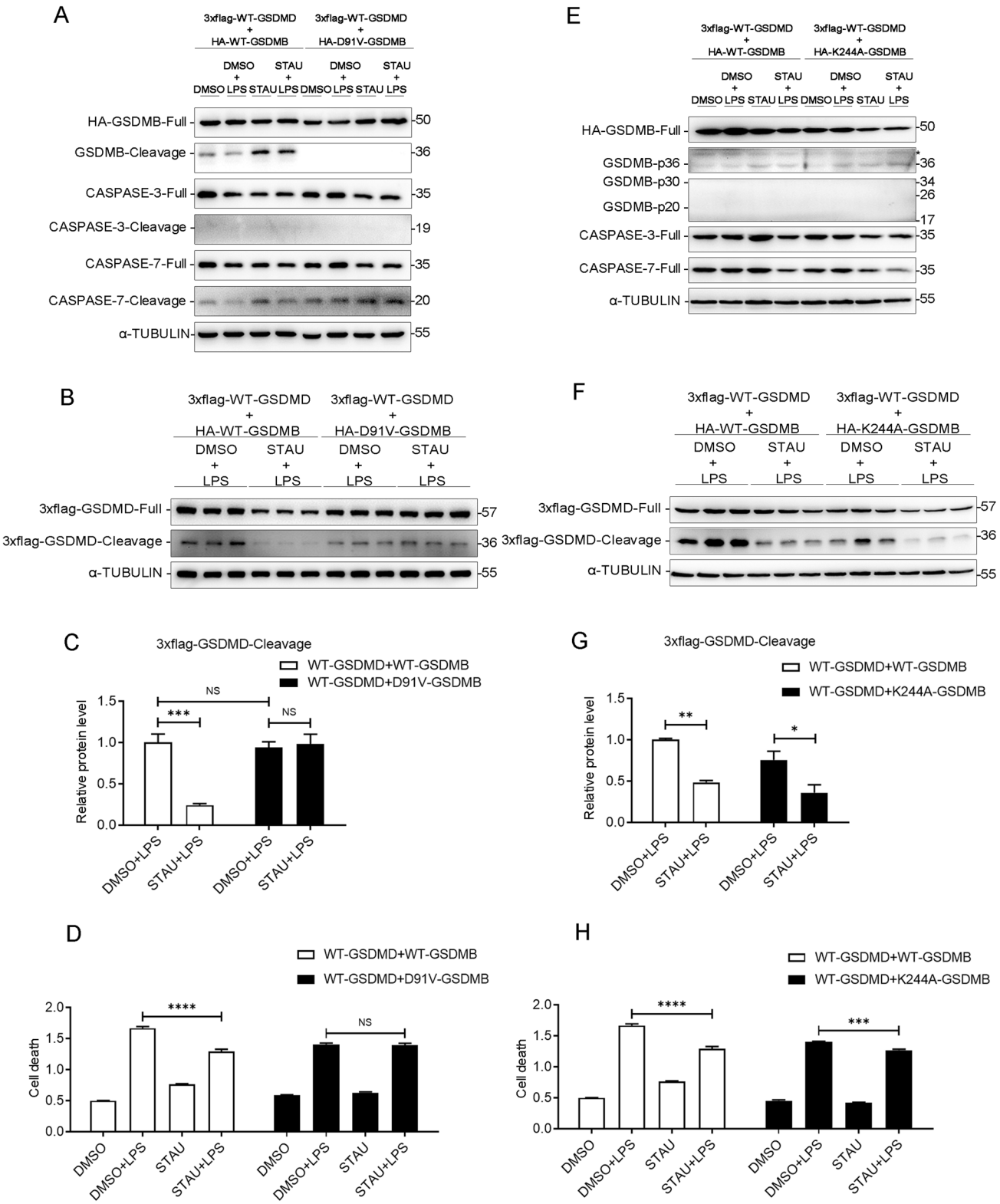

checked the mRNA levels and protein levels of GSDMB in different tissues of WT mice and GSDMB-transgenic mice. Consistently, GSDMB is mainly expressed in the gastrointestinal tract of mice including small intestine, colon and stomach (Supplementary Fig. 8C, D), which is similar to the expression profile in humans [32]. GSDMB was expressed in the immune cells of GSDMB-transgenic mice (Supplementary Fig. 8B, E). Bone marrow-derived macrophages (BMDMs) from GSDMB-transgenic mice were more sensitive to *E. coli* than those from WT mice. The cleavage of GSDMD and caspase-11 was enhanced during *E. coli* infection (Supplementary Fig. 8E). Consistently, there were more pyroptotic GSDMB-transgenic BMDMs during *E. coli* infection (Supplementary Fig. 8F and Supplementary Movie 2). These results suggest that consistent with humans, the GSDMB-enhanced pyroptosis

Fig. 4 Caspase-7-mediated GSDMB cleavage is necessary for the apoptotic inhibition of non-canonical pyroptosis. A–D HeLa cells were transfected with 3xflag-WT-GSDMD and HA-WT-GSDMB or HA-D91V-GSDMB (empty vector as control), after 24 h, cells were treated with 8 μM STAU (DMSO as control) for 3.5 h and then electrically transferred LPS to induce non-canonical pyroptosis. **A** Immunoblotting for CASPASE-3-Full, CASPASE-7-Full, CASPASE-3-Cleavage, CASPASE-Cleavage, HA-GSDMB-Full and GSDMB-Cleavage in whole cell lysates. α-TUBULIN is used as a loading control. **B** Immunoblotting for 3xflag-GSDMD-Full and 3xflag-GSDMD-Cleavage in whole cell lysates. α-TUBULIN is used as a loading control. **C** The gray scale analysis of 3xflag-GSDMD-Cleavage/3xflag-GSDMD-Full in (**B**). **D** LDH assay for cell death in indicated HeLa cells. **E–H** HeLa cells were transfected with 3xflag-WT-GSDMD and HA-WT-GSDMB or HA-K244A-GSDMB, after 24 h, cells were treated with 8 μM STAU (DMSO as control) for 3.5 h and then electrically transferred LPS to induce non-canonical pyroptosis. **E** Immunoblotting for HA-GSDMB-Full, GSDMB-p20, GSDMB-p30, GSDMB-p36, CASPASE-3-Full and CASPASE-7-Full in whole cell lysates. α-TUBULIN is used as a loading control. GSDMB-p20 (92-244aa) was generated by D91 cleavage by CASPASE-3/7 and by K244 cleavage by GZMA. GSDMB-p30 (1-244aa) was generated by K244 cleavage by GZMA. GSDMB-p36 (92-417aa) was generated by D91 cleavage by CASPASE-3/7. Non-specific bands are indicated with an asterisk (*). **F** Immunoblotting for 3xflag-GSDMD-Full and 3xflag-GSDMD-Cleavage in whole cell lysates. α-TUBULIN is used as a loading control. **G** The gray scale analysis of 3xflag-GSDMD-Cleavage/3xflag-GSDMD-Full in (**F**). **H** LDH assay for cell death in indicated HeLa cells. Each panel is a representative experiment of at least three replicates. Data are presented as the mean ± SD. **C**, **D**, **G**, and **H** ANOVA followed by Bonferroni's post-test: *$p < 0.05$, **$p < 0.01$, ***$p < 0.001$,****$p < 0.0001$, NS = not significant. Full = full length. All the HA-tagged proteins were detected with anti-HA antibodies. All the 3xflag-tagged proteins were detected with anti-flag antibodies. Unlabeled GSDMB proteins were detected with anti-GSDMB antibodies.

pathway is significantly activated during *E. coli* infection in GSDMB-transgenic BMDMs from mice.

We also found the increased cleavage of Caspase-3, Caspase-7 and GSDMB in GSDMB-transgenic BMDMs during *E. coli* infection, suggesting that apoptotic inhibition of noncanonical pyroptosis may also occur in GSDMB-transgenic mice (Supplementary Fig. 8E). The release of IL-1β and LDH was significantly increased when caspase-7 was inhibited by inhibitor Z-DEVD-FMK in GSDMB-transgenic BMDMs (Supplementary Fig. 9A, B). Furthermore, the live-cell imaging data showed that there were more pyroptotic cells when caspase-7 was inhibited during *E. coli* infection (Supplementary Fig. 9C and Supplementary Movie 3). Furthermore, we constructed the GSDMB-transgenic + *Caspase7*-KO mice to analysis cell death of BMDMs during bacterial infection. The *Caspase11*-KO mice were used as the negative control. The secretion of IL-1β significantly increased when caspase-7 was knockout during *E. coli* infection (Fig. 7F). Correspondingly, the live-cell imaging results showed that more pyroptotic cells were observed during persistent infection with *E. coli* in the GSDMB-transgenic + *Caspase7*-KO group than in the other group (Fig. 7G and Supplementary Movie 4). Overall, apoptotic caspase-7 activation inhibits noncanonical pyroptosis during bacterial infection in GSDMB-transgenic BMDMs.

We explored the role of the caspase-7-GSDMB axis in regulating caspase-4 and noncanonical pyroptosis after infection of the sepsis-inducing *S. Typhimurium* in human THP-1 cells. *CASPASE-4/5* knockdown THP-1 cells were used as the negative control. The GSDMD cleavage, caspase-4 cleavage and IL-1β release were both inhibited in *CASPASE-4/5* knockdown THP-1 cells compared with those of WT cells, suggesting that S. Typhimurium infection could induce CASPASE-4/5-mediated noncanonical pyroptosis pathway (Supplementary Fig. 8G, H, J). The cleavage of GSDMD and CASPASE-4 was enhanced during *S. Typhimurium* infection in *CASPASE-7* knockdown THP-1 cells (Supplementary Fig. 8G, H). Consistently, the release of IL-1β was significantly upregulated in *CASPASE-7* knockdown THP-1 cells (Supplementary Fig. 8J). Furthermore, knockdown of *CASPASE-7* significantly inhibited the cleavage of GSDMB, suggesting that *CASPASE-7* knockdown enhanced GSDMB full length-mediated noncanonical pyroptosis during S. Typhimurium infection (Supplementary Fig. 8G, I). These results suggest that CASPASE-7-mediated apoptosis inhibits noncanonical pyroptosis during *S. Typhimurium* infection in THP-1 cells.

To explore the physiological role of GSDMB in vivo, we generated a septic model by two consecutive intraperitoneal injections of LPS, which primarily activated the noncanonical pyroptosis pathway [33–35]. Compared to WT mice, GSDMB-transgenic mice showed a lower survival rate, higher secretion of IL-1β and more severe lung lesions (Supplementary Fig. 9D–F). These results suggest that GSDMB promotes noncanonical pyroptosis in vivo. Next, we explored whether the septic mice had spontaneously activated Caspase-7 and subsequent inhibition of the GSDMB-mediated proinflammatory pathway. As expected, the immunoblot results showed that Caspase-7 was significantly activated in both WT septic mice and GSDMB-transgenic septic mice (Supplementary Fig. 9G). Furthermore, GSDMB-transgenic mice that were pretreated with the caspase-7 inhibitor Z-DEVD-FMK showed a decreased survival rate, suggesting that inhibition of caspase-7 significantly exacerbated sepsis (Supplementary Fig. 9H). These results supported our conclusion that the cleavage of GSDMB by caspase-7 alleviate the noncanonical pyroptosis.

Next, we confirmed the function of caspase-7 in septic GSDMB-transgenic + *Caspase7*-KO mice. Compared to GSDMB-transgenic mice, GSDMB-transgenic + *Caspase7*-KO mice showed a lower survival rate and more severe lung lesions in septic models (Fig. 7H, I). We found that the WT + *Caspase7*-KO mice showed a more severe septic phenotype compared to the WT mice (Fig. 7H, I), suggesting that Caspase-7 expression might be beneficial for mice and the mice that completely lack Caspase-7 are more susceptible to sepsis. A study reported that activated caspase-7 could cleave acid sphingomyelinase and promote the repair of pyroptotic pores, which ameliorates tissue pathology during *S. Typhimurium* infection [36]. In summary, apoptotic inhibition of noncanonical pyroptosis is dependent on the caspase7/GSDMB axis and is a self-protective pathway to avoid overactivation of inflammation during bacterial infection.

DISCUSSION

The balance between apoptosis and pyroptosis is important for inflammatory diseases, such as sepsis. Current studies of sepsis have focused on targeting a specific gene to alleviate sepsis. An antibody strategy targeting the TN/HMGB1 interaction and knockout of caspase-12 or miR-221/222 can alleviate sepsis [37–39]. The TLR4 inhibitors TAK-242 and parthenolide reduce the levels of inflammatory factors and protect septic mice [40, 41]. The IL-17 receptor blocking antibody inhibits IL-18-mediated toxicity and relieves sepsis [42]. Anakinra inhibits the IL-1 receptor and improves the survival of septic patients [43]. In this paper, we focused on the regulatory effect of apoptosis on noncanonical pyroptosis, which might indicate new therapeutic targets for sepsis in the future.

Caspase-7 plays an important role in the balance between apoptosis and noncanonical pyroptosis. Activated caspase-7 can cleave GSDMB at the D91 site during apoptosis. Cleaved GSDMB (92-417 aa) blocked the interaction between GSDMB (1-91 aa) and caspase-4 to inhibit noncanonical pyroptosis (Fig. 5). GSDMD can be cleaved by activated caspase-3/7 at the D87 site and produce

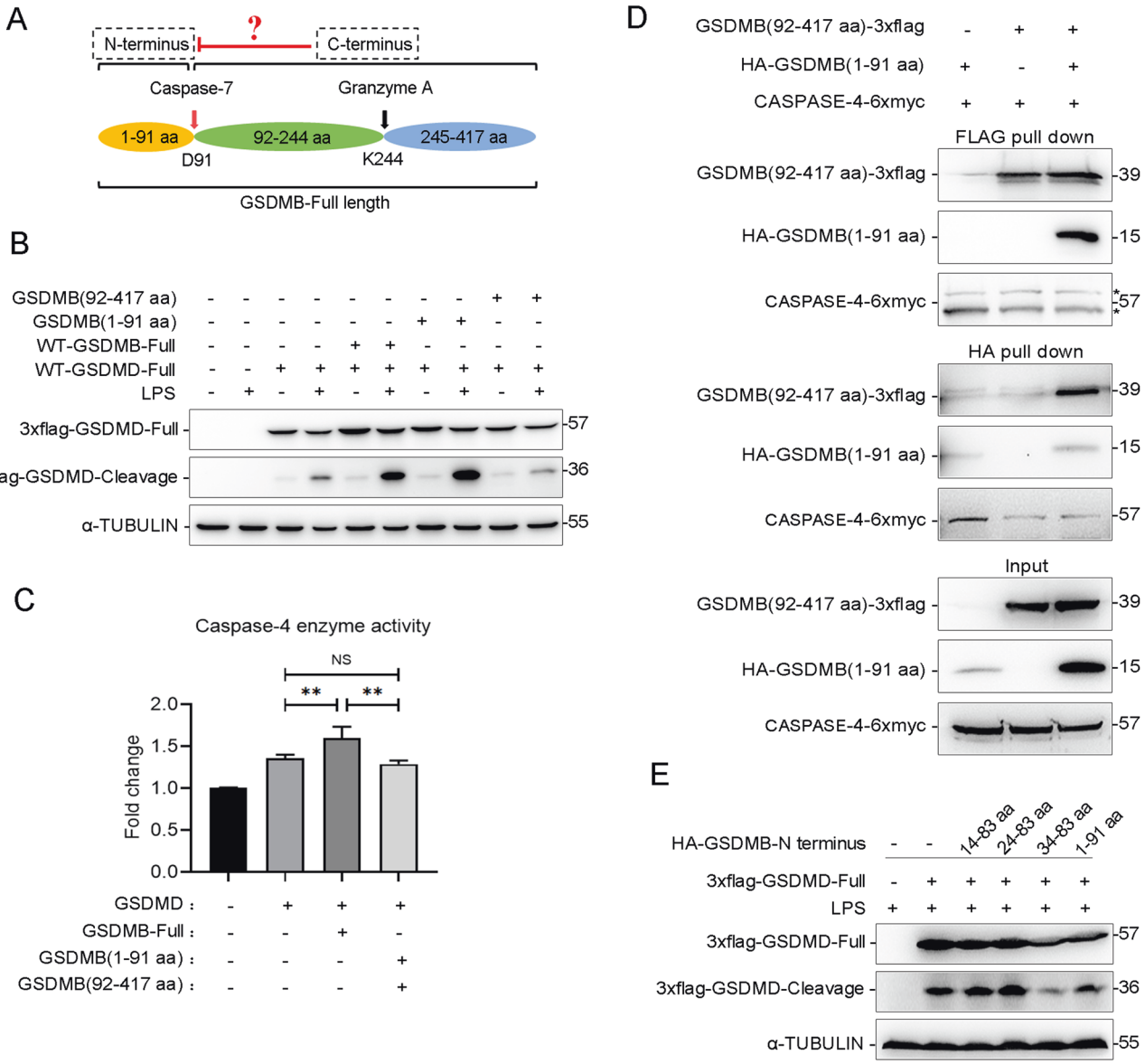

Fig. 5 GSDMB cleaved at D91 site cannot promote the enzyme activity of caspase-4. A The schematic diagram of GSDMB cleavage. GSDMB can be cleaved at D91 by CASPASE-7 and at K244 by granzyme A to produce the GSDMB (1-91aa), GSDMB (92-244aa) and GSDMB (245-417aa). **B** Immunoblotting for 3xflag-GSDMD-Full and 3xflag-GSDMD-Cleavage in whole cell lysates. α-TUBULIN is used as a loading control. HeLa cells were transfected with the indicated plasmids, after 24 h, cells were electrically transferred LPS to induce non-canonical pyroptosis. **C** The CASPASE-4 enzyme activity of indicated cells was examined. HeLa cells were transfected with the indicated plasmids, after 24 h, cells were electrically transferred LPS to induce non-canonical pyroptosis. **D** Co-immunoprecipitations with the anti-FLAG antibody and anti-HA antibody of whole-cell extracts from HEK293T cells transfected with the indicated plasmids. Immunoblotting was performed using the indicated antibodies. Non-specific bands are indicated with an asterisk (*). **E** Immunoblotting for 3xflag-GSDMD-Full and 3xflag-GSDMD-Cleavage in whole cell lysates. α-TUBULIN is used as a loading control. HeLa cells were transfected with 3xflag-GSDMD-Full and indicated truncated plasmids of GSDMB (empty vector as control), after 24 h, cells were electrically transferred LPS to induce non-canonical pyroptosis. Each panel is a representative experiment of at least three replicates. Data are presented as the mean ± SD. **C** ANOVA followed by Bonferroni's post-test: $^{**}p < 0.01$, NS = not significant. Full = full length. All the HA-tagged proteins were detected with anti-HA antibodies. All the 3xflag-tagged proteins were detected with anti-flag antibodies. All the Myc-tagged proteins were detected with anti-Myc antibodies.

nontoxic N-terminal fragments [23, 24]. However, apoptotic inhibition of noncanonical pyroptosis was independent of this pathway in HeLa cells (Supplementary Fig. 6). There are two possibilities for this result. First, previous studies that the D87 site of GSDMD cleaved by apoptotic caspases inhibited pyroptosis performed only in vitro experiments [23, 24]. A recent report suggests that the cleavage of GSDMD by activated caspase-3/7 does not suppress pyroptosis in vivo [25]. Second, the apoptotic cleavage of GSDMD may not be strong enough to block the toxic effects of the GSDMD N-terminus.

GSDME did not affect the apoptotic inhibition of noncanonical pyroptosis (Supplementary Fig. 7). Compared with caspase-3, the main downstream substrate of caspase-7 may be GSDMB rather than GSDME during apoptosis in THP-1 cells. Furthermore, GSDME is not highly expressed in THP-1 cells. Therefore, the GSDME-related pyroptosis pathway does not function robustly, or GSDME-mediated pores are repaired by membrane repair proteins, such as the ESCRT-III complex.

The K244 site of GSDMB can be cleaved by granzyme A released from natural killer cells and cytotoxic T lymphocytes. The toxic

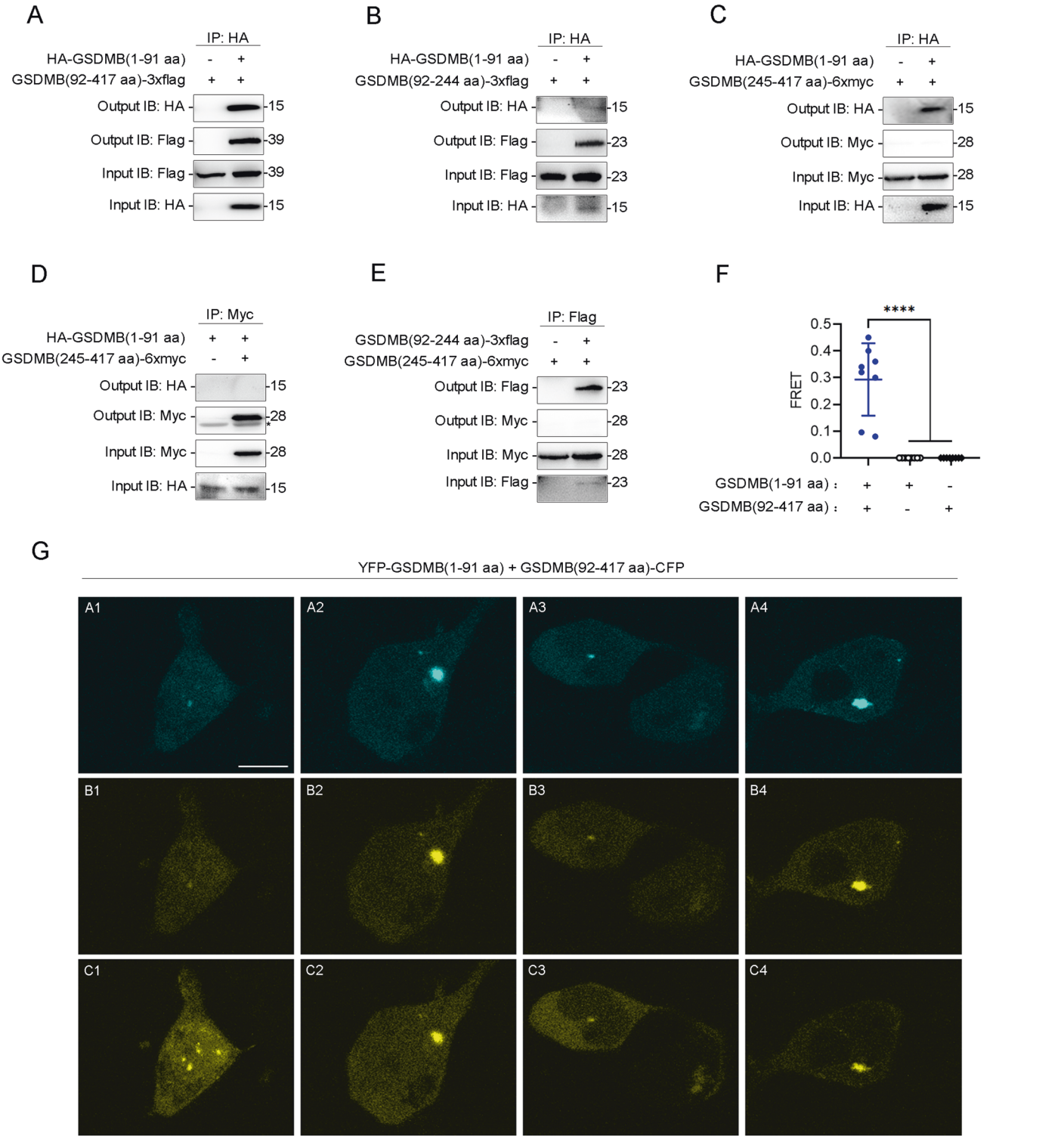

Fig. 6 GSDMB C-terminus (92-417 aa) can bind to GSDMB N-terminus (1-91 aa) to block its function. A–E Co-immunoprecipitations with the anti-FLAG antibody or anti-HA antibody or anti-Myc antibody of whole-cell extracts from HEK293T cells transfected with the indicated plasmids. Immunoblotting was performed using the indicated antibodies. Non-specific bands are indicated with an asterisk (*). **F** The quantification of FRET efficiency of HEK293T cells expressing the indicated plasmids. $n = 8$ per group. **G** The representative FRET images of HEK293T cells co-expressing YFP-GSDMB (1-91aa) and GSDMB (92-417aa)-CFP. Bar = 10 μm. These images were taken by Leica SP5. **A** donor emission, **B** FRET, **C** acceptor emission. Data are presented as the mean ± SD. **F** ANOVA followed by Bonferroni's post-test: ****$p < 0.0001$. All the HA-tagged proteins were detected with anti-HA antibodies. All the 3xflag-tagged proteins were detected with anti-flag antibodies. All the Myc-tagged proteins were detected with anti-Myc antibodies.

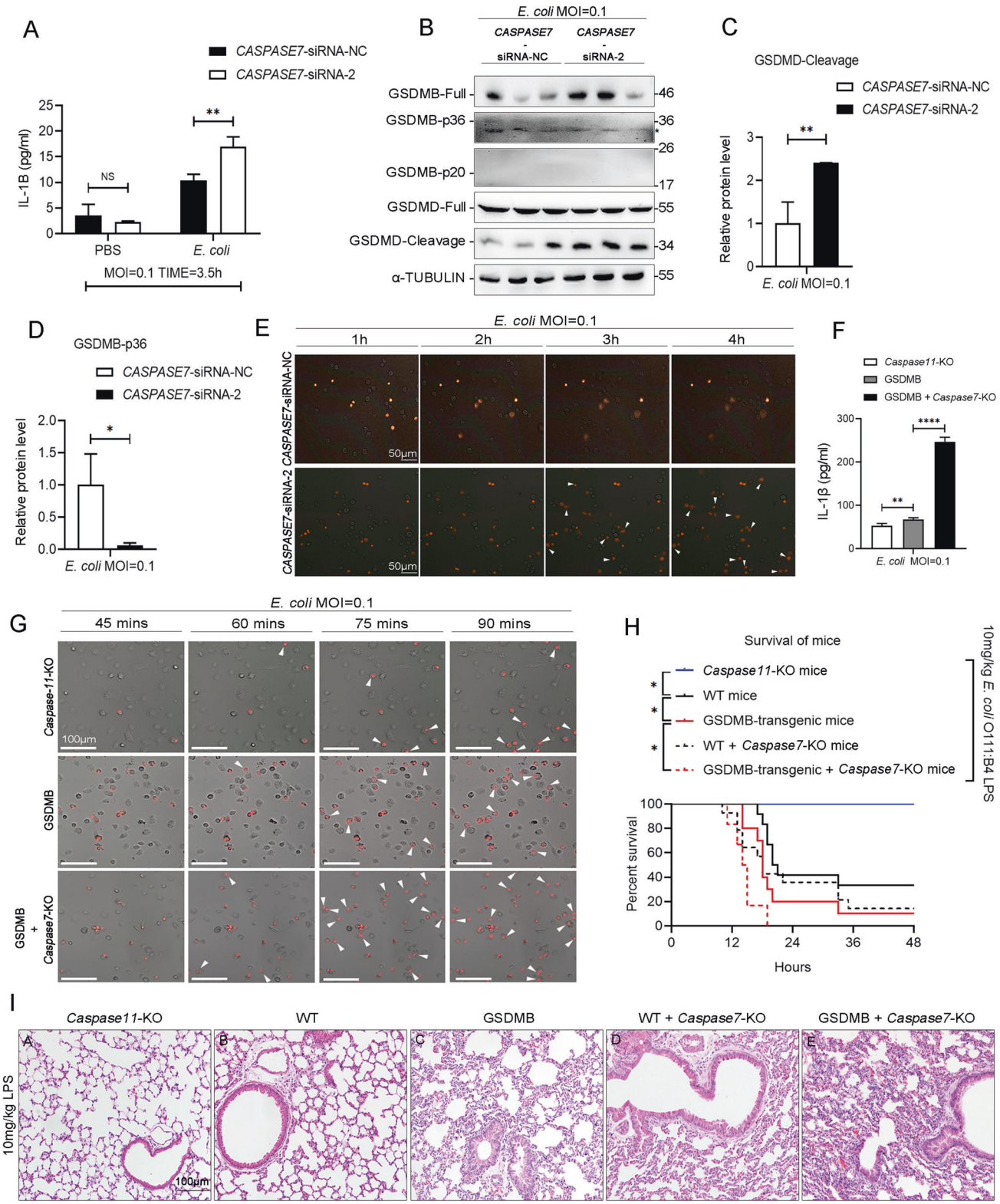

N-terminal fragment can perforate the cell membrane to induce pyroptosis [7]. We found that the granzyme A/GSDMB pathway was activated in the lungs of sterile septic mice and the PBMCs of septic patients (data not shown). These results might suggest that GSDMB-mediated toxic effects during sepsis were dependent not only on the GSDMB (1-91 aa) -mediated noncanonical pyroptosis pathway but also on the GSDMB (1-244 aa) -mediated pyroptosis pathway. In PBMCs from septic shock patients, the granzyme A/GSDMB pathway was significantly inhibited, while the caspase-7/GSDMB pathway was significantly activated (data not shown). We suspect that apoptotic caspase-7-related GSDMB cleavage not only directly destroys toxic GSDMB (1-244 aa) but also activates GSDMB (92-417 aa)-mediated inhibition of noncanonical pyroptosis. Finally, activated caspase-7 alleviates these GSDMB-

Fig. 7 Apoptotic inhibition of non-canonical pyroptosis is a self-protective pathway during bacterial infection. A–E THP-1 cells were electrically transferred control siRNA (*CASPASE7*-siRNA-NC) and *CASPASE7* siRNA (*CASPASE7*-siRNA-2). After 45 h, cells were incubated with *E. coli* (MOI = 0.1) for indicated time at 37°C (PBS as control). **A** IL-1β release from indicated THP-1 cells was measured by ELISA. **B** Immunoblotting for GSDMB-Full, GSDMD-Full, GSDMD-Cleavage, GSDMB-p20 and GSDMB- p36 in whole cell lysates. α-TUBULIN is used as a loading control. GSDMB-p20 (92-244aa) was generated by D91 cleavage by CASPASE-3/7 and by K244 cleavage by GZMA. GSDMB-p36 (92-417aa) was generated by D91 cleavage by CASPASE-3/7. Non-specific bands are indicated with an asterisk (*). **C** The gray scale analysis of GSDMD-Cleavage/GSDMD-Full in (**B**). **D** The gray scale analysis of GSDMB-p36/GSDMB-Full in (**B**). **E** Data show representative time-course live cell images (brightfield and fluorescence). Loss of membrane integrity was indicated by PI (red) staining of nuclear DNA. Representative pyroptotic cells are indicated with white arrows. Bar = 50 μm. **F, G** Primary BMDMs from 10 ~ 12-week-old *Caspase11*-KO, GSDMB-transgenic and GSDMB-transgenic + *Caspase7*-KO mice were incubated with *E. coli* (MOI = 0.1) for indicated time at 37°C (PBS as control). **F** IL-1β release from indicated BMDMs was measured by ELISA at 7 h after infection. **G** Data show representative time-course live cell images (brightfield and fluorescence). Loss of membrane integrity was indicated by PI (red) staining of nuclear DNA. Representative increased pyroptotic cells are indicated with white arrows. Bar = 100 μm. **H, I** 10 ~ 12-week-old WT (C57BL/6 J), GSDMB-transgenic, WT + *Caspase7*-KO, GSDMB-transgenic + *Caspase7*-KO and *Caspase11*-KO male mice were intraperitoneally primed with 0.4 mg/kg *E. coli* O111:B4 LPS, then challenged with 10 mg/kg *E. coli* O111:B4 LPS intraperitoneally (0.9% NaCl as control) after 6 h. **H** Survival of indicated septic mice. WT mice: $n = 12$, GSDMB-transgenic mice: $n = 10$, WT + *Caspase7*-KO mice: $n = 14$, GSDMB-transgenic + *Caspase7*-KO mice: $n = 6$, *Caspase11*-KO mice: $n = 5$. **I** Representative lung sections stained with H&E from the indicated mice at 10 h after LPS challenge. Bar = 100 μm. Each panel is a representative experiment of at least three replicates. Data are presented as the mean ± SD. **A, F** ANOVA followed by Bonferroni's post-test: $^{**}p < 0.01$, $^{****}p < 0.0001$, NS = not significant. **C, D** *T*-test: $^{*}p < 0.05$, $^{**}p < 0.01$. **H** Gehan–Breslow–Wilcoxon test: $^{*}p < 0.05$. Full = full length. Endogenous GSDMB proteins were detected with anti-GSDMB antibodies.

mediated toxic effects and achieves self-protection. However, this hypothesis needs further verification.

In addition to caspase-7, many studies have reported that other members of the caspase family play roles in the balance between pyroptosis and apoptosis. Activation of caspase-3 through endogenous and exogenous apoptotic pathways cleave GSDME to promote pyroptosis [27]. Caspase-3 is activated *via* the mitochondrial apoptotic proteins BAX/BAK and promotes caspase-8-related cleavage of IL-1β and potassium efflux-related NLRP3 inflammasome assembly [44]. Caspase-3 and caspase-7 have great sequence similarity compared to other mammalian caspase family members, but they are functionally different enzymes; caspase-3 is the major apoptosis-associated effector [45]. The current experimental conclusions about the regulation of apoptosis and pyroptosis by caspase-3/7 are still very controversial. Therefore, caspase-3 and caspase-7 may rely on different mechanisms and have different effects on the balance of apoptosis and pyroptosis, which needs to be further identified.

Caspase-8 plays an important role in the exogenous apoptotic pathway and can cleave caspase-3/7 to promote apoptosis. Several studies have shown that caspase-8 is also involved in the regulation of the pyroptosis pathway. Activated NLRP3 induced by caspase-8-related alternative inflammatory pathways promotes the maturation of the inflammatory factor IL-1β [46]. The RIPK1/RIPK3-related pathway activates the NLRP3 inflammasome and promotes the release of IL-1β in caspase-8-deficient dendritic cells [47]. Blocking the catalytic activity of caspase-8 can activate ASC/caspase-1-related inflammatory pathways and promote the secretion of IL-1β, which induces perinatal lethality in MLKL-deficient mice [48]. Activated caspase-8 also induces the GSDMC-mediated pyroptosis pathway [49]. Furthermore, caspase-8 promotes pyroptosis by inducing the cleavage of GSDMD [50]. Caspase-8 activation is mediated by the exogenous apoptotic pathway and drives NLRP3 inflammasome assembly by activating pannexin-1 [51]. During influenza A virus infection, caspase-8 can activate caspase-1 and caspase-3 to induce the activation of both apoptotic and pyroptotic pathways [52]. Overall, caspase-8 plays a critical role in both the apoptotic and pyroptotic pathways.

Caspase-1 is a key factor in canonical pyroptosis. However, activated caspase-1 promotes apoptosis when the canonical pyroptosis pathway is blocked. Activated caspase-1 activates caspase-3/7 to induce apoptosis in GSDMD-knockout cells after stimulation with pyroptotic reagents [24]. Activated caspase-1 cleaves GSDMD and produces a toxic N-terminal fragment, which perforates the mitochondrial membrane to promote apoptotic body-mediated endogenous apoptotic pathways [53]. ASC induces apoptosis in caspase-1-deficient macrophages after stimulation with NLRP3 and AIM2 agonists [54]. The pyroptosis-associated NLRP1b and NLRC4 inflammasomes promote apoptosis in caspase-1-deficient macrophages [55]. During NLRP3 and AIM2 inflammasome activation, ASC can bind to pro-caspase-1 and pro-caspase-8 through different regions to induce the activation of both apoptotic and pyroptotic pathways, and knockdown of caspase-1 induces more apoptosis in cells [56]. Caspase-7 but not caspase-3 is an important substrate of activated caspase-1 in response to microbial stimuli and bacterial infection [57]. Caspase-11 is a critical initiator caspase in noncanonical pyroptosis. However, it can activate caspase-3 efficiently in a mouse model of stroke [58]. Overall, the key caspases associated with pyroptosis also trigger apoptosis.

Current studies have shown that caspase family members may have potential roles in the regulation of apoptosis and pyroptosis. However, the relevant mechanisms are still controversial and depend on the cell type. Therefore, analyzing the specific regulatory mechanism of caspase family members in different cell types is necessary. It may help us to identify potential therapeutic targets to reduce inflammation and treat inflammatory disease.

In conclusion, full-length GSDMB can bind to caspase-4 *via* its N-terminus (1-91 aa) and enhance enzymatic activity during noncanonical pyroptosis. Based on this, GSDMB may be a proinflammatory factor in sepsis. Activated caspase-7 can cleave GSDMB at D91 to block GSDMB-mediated promotion of non-canonical pyroptosis. Mechanistically, the cleaved GSDMB-C-terminus (92-417 aa) binds to the GSDMB-N-terminus (1-91 aa) and then inhibits the function of the N-terminus. Furthermore, the survival rates were significantly decreased when apoptosis was inhibited in septic GSDMB-transgenic mice. Thus, caspase-7/GSDMB-related apoptotic inhibition of noncanonical pyroptosis is a self-protective pathway to avoid overactivation of inflammation during bacterial infection (Fig. 8). Moreover, this pathway provides potential therapeutic targets for sepsis in the future.

MATERIALS AND METHODS

Cell culture

THP-1 cells (Shanghai Institute of Cell Biology) were cultured in RPMI 1640 medium. HEK293T cells (ATCC), HeLa cells (ATCC), primary BMDMs were cultured in DMEM medium. All mediums were supplemented with 10% fetal bovine serum (FBS, PAN Biotech) and 1% penicillin/streptomycin. All cells mentioned above were grown at 37 °C and 5% CO_2 and were negative for mycoplasma test (#D101-02, Vazyme).

Plasmids and transfection

Complementary DNA (cDNA) for human *GSDMD*, *GSDME* and *GSDMB* was amplified from reverse-transcribed cDNA from THP-1 cells. cDNA for

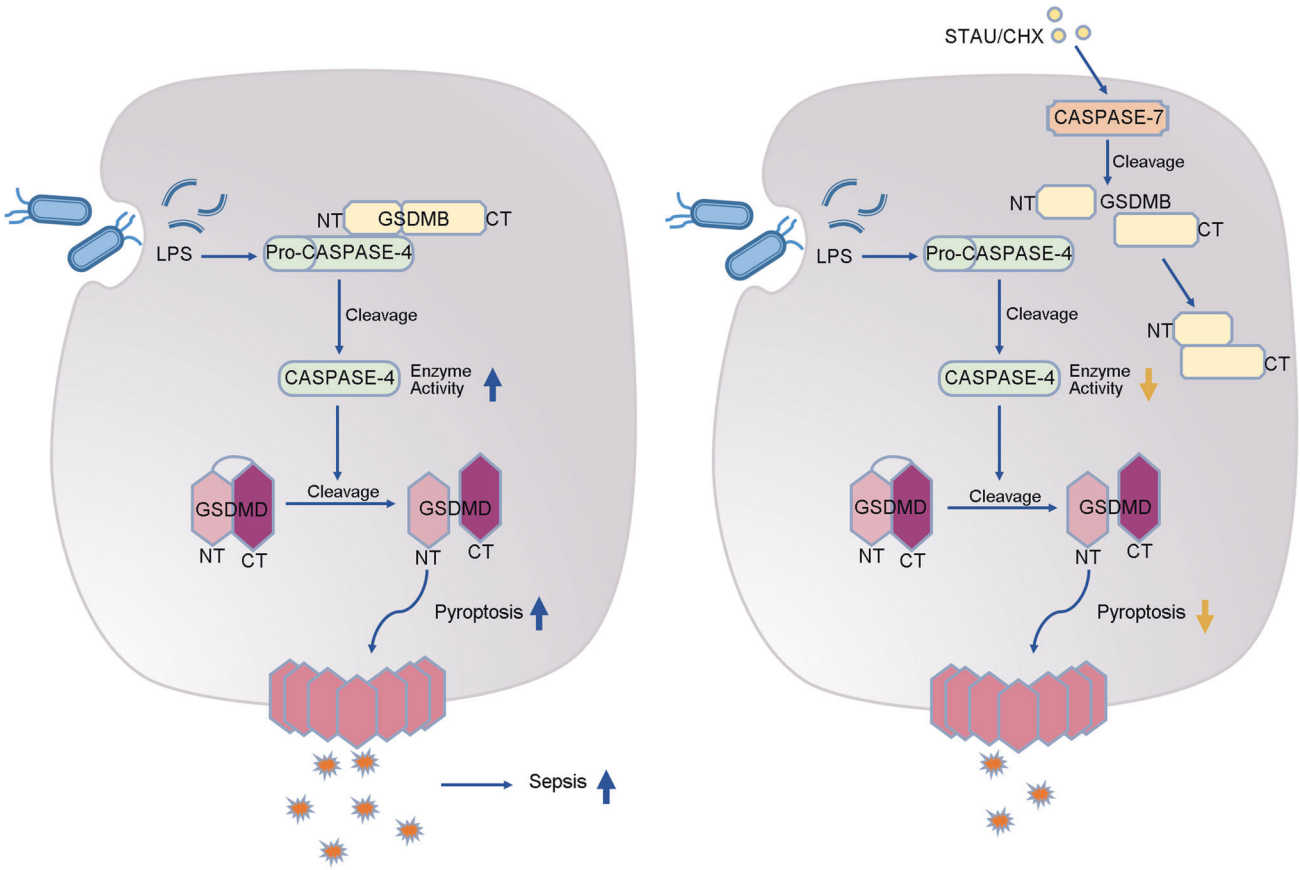

Fig. 8 Conclusion. Apoptotic caspase-7 activation inhibits non-canonical pyroptosis *via* GSDMB cleavage.

human *CASPASE3*, *CASPASE4* and *CASPASE7* was kindly provided by Prof. Jiahuai Han from Xiamen University, China. The other cDNAs were constructed by PCR amplification. The detail construction was provided in Supplementary information. All plasmids were identified by PCR and DNA sequencing. All plasmids were transfected followed the instructions of Lipofectamine 2000 Transfection Reagent (Invitrogen).

siRNA knockdown

Human *CASPASE3*, *CASPASE7*, *CASPASE6*, *CASPASE8*, *CASPASE4/5* and *GSDME* siRNAs were purchased from GenePharma (Table S1). The Neon™ Transfection System 10 μL/100 μL Kit (#MPK1096, Invitrogen) was used for electric transfection. The details were provided in Supplementary information.

Activation of apoptosis and non-canonical pyroptosis

Staurosporine (#HY-15141, MCE) and cycloheximide (#HY-12320, MCE) were used to activate apoptosis. The Neon™ Transfection System 10 μl/100 μl Kit (#MPK1096, Invitrogen) was used to induce non-canonical pyroptosis by LPS electroporation. The details were provided in Supplementary information.

Measurement of LDH release, caspase-4 enzyme activity, and IL-1β

CytoTox 96® Non-Radioactive Cytotoxicity Assay (#G1782, Promega) was used to detect LDH release. The Caspase-4 Assay kit (#ab65659, Abcam) was used to measure caspase-4 enzyme activity following the instructions. The Human IL-1beta ELISA Kit (#FMS-ELH002, FcMACS) and the Mouse IL-1β ELISA Kit (#FMS-ELM002, FcMACS) were used to measure IL-1β of cell culture supernatant or mouse serum following the instructions of manufacturers. The details were provided in Supplementary information.

Immunoblotting and antibodies

Detailed methods and antibodies were provided in Supplementary information.

FRET assay

YFP- and CFP- tagged plasmids were transfected into HEK293T cells that had been plated at 30–40% density on confocal dishes. The images of the FRET assay were taken and analyzed by a Leica SP5 system. The procedures were performed according to FRET Sensitized Emission (SE) in LASAF (Leica Microsystems Inc).

Bacterial infection experiments

Escherichia coli (#CICC 10003, China Center of Industrial Culture Collection) was cultured in LB liquid medium at 37 °C. *S. Typhimurium* (#SL-1344 bio-110940, Nanjing juxiong Hua Biotechnology Co., Ltd) was cultured in LB solid medium at 37 °C. The details were provided in Supplementary information.

Animal studies

GSDMB-transgenic mice in C57BL/6 J background were generated by the Nanjing Biomedical Research Institute (NBRI) of Nanjing University. C57BL/6 J mice, *Caspase7*-KO mice and GSDMB-transgenic + *Caspase7*-KO mice were provided by the Model Animal Research Center (MARC) of Nanjing University. *Caspase11*-KO mice were kindly provided by Prof. Shu Zhu from University of Science and Technology of China. Mice were randomly allocated into their respective groups (non-blinded).

The procedures of construction of LPS-induced septic mouse model, H&E staining, and extraction of primary BMDMs were provided in Supplementary information.

Co-immunoprecipitation experiments

The indicated HA-, Flag-, Myc-tagged plasmids were transfected into HEK293T cells. The details were provided in Supplementary information.

Statistics

Sample size (*n*), performed statistical analyses and statistical significance are stated in the figure legends. No statistical tests were used to estimate

sample size. No sample or animal was excluded from the analysis. GraphPad Prism 8.0.1 was used to quantize LDH and IL-1β release, FRET efficiency, caspase-4 enzyme activity, mouse survival and FACS data. ImageJ 1.8.0 was used to quantize the gray scale analysis of immunoblotting. Mouse survival was analyzed statistically by Gehan–Breslow–Wilcoxon test. The student *t*-test was used to analyze the data between the two groups and the ANOVA with post hoc correction (Bonferroni's post-test and Holm-Sidak's post-test) was used to multi-group analysis. $^{*}p < 0.05$, $^{**}p < 0.01$, $^{***}p < 0.001$, $^{****}p < 0.0001$, NS = not significant.

DATA AVAILABILITY

The data sets used in the current study are available from the corresponding author upon reasonable request. The western blot data are provided in Supplementary Materials (Original western blots).

REFERENCES

1. He H, Yi L, Zhang B, Yan B, Xiao M, Ren J, et al. USP24-GSDMB complex promotes bladder cancer proliferation via activation of the STAT3 pathway. Int J Biol Sci. 2021;17:2417–29.
2. Carl-McGrath S, Schneider-Stock R, Ebert M, Röcken C. Differential expression and localisation of gasdermin-like (GSDML), a novel member of the cancer-associated GSDMDC protein family, in neoplastic and non-neoplastic gastric, hepatic, and colon tissues. Pathology. 2008;40:13–24.
3. Molina-Crespo Á, Cadete A, Sarrio D, Gámez-Chiachio M, Martinez L, Chao K, et al. Intracellular delivery of an antibody targeting gasdermin-B reduces HER2 breast cancer aggressiveness. Clin Cancer Res. 2019;25:4846–58.
4. Söderman J, Berglind L, Almer S. Gene expression-genotype analysis implicates GSDMA, GSDMB, and LRRC3C as contributors to inflammatory bowel disease susceptibility. Biomed Res Int. 2015;2015:834805.
5. Li X, Christenson SA, Modena B, Li H, Busse WW, Castro M, et al. Genetic analyses identify GSDMB associated with asthma severity, exacerbations, and antiviral pathways. J Allergy Clin Immunol. 2021;147:894–909.
6. Chen Q, Shi P, Wang Y, Zou D, Wu X, Wang D, et al. GSDMB promotes non-canonical pyroptosis by enhancing caspase-4 activity. J Mol Cell Biol. 2019;11:496–508.
7. Zhou Z, He H, Wang K, Shi X, Wang Y, Su Y, et al. Granzyme A from cytotoxic lymphocytes cleaves GSDMB to trigger pyroptosis in target cells. Science. 2020;368:eaaz7548.
8. Hansen JM, de Jong MF, Wu Q, Zhang LS, Heisler DB, Alto LT, et al. Pathogenic ubiquitination of GSDMB inhibits NK cell bactericidal functions. Cell. 2021;184:3178–91.e18.
9. Broz P, Ruby T, Belhocine K, Bouley DM, Kayagaki N, Dixit VM, et al. Caspase-11 increases susceptibility to Salmonella infection in the absence of caspase-1. Nature. 2012;490:288–91.
10. Rathinam VA, Vanaja SK, Waggoner L, Sokolovska A, Becker C, Stuart LM, et al. TRIF licenses caspase-11-dependent NLRP3 inflammasome activation by gram-negative bacteria. Cell. 2012;150:606–19.
11. Liu Q, Zhang S, Sun Z, Guo X, Zhou H. E3 ubiquitin ligase Nedd4 is a key negative regulator for non-canonical inflammasome activation. Cell Death Differ. 2019;26:2386–99.
12. Song F, Hou J, Chen Z, Cheng B, Lei R, Cui P, et al. Sphingosine-1-phosphate receptor 2 signaling promotes caspase-11-dependent macrophage pyroptosis and worsens Escherichia coli sepsis outcome. Anesthesiology. 2018;129:311–20.
13. Ashida H, Mimuro H, Ogawa M, Kobayashi T, Sanada T, Kim M, et al. Cell death and infection: a double-edged sword for host and pathogen survival. J Cell Biol. 2011;195:931–42.
14. Chao KL, Kulakova L, Herzberg O. Gene polymorphism linked to increased asthma and IBD risk alters gasdermin-B structure, a sulfatide and phosphoinositide binding protein. Proc Natl Acad Sci USA. 2017;114:E1128–E37.
15. Belmokhtar CA, Hillion J, Ségal-Bendirdjian E. Staurosporine induces apoptosis through both caspase-dependent and caspase-independent mechanisms. Oncogene. 2001;20:3354–62.
16. Johansson AC, Steen H, Ollinger K, Roberg K. Cathepsin D mediates cytochrome c release and caspase activation in human fibroblast apoptosis induced by staurosporine. Cell Death Differ. 2003;10:1253–9.
17. Schwarz N, Tumpara S, Wrenger S, Ercetin E, Hamacher J, Welte T, et al. Alpha1-antitrypsin protects lung cancer cells from staurosporine-induced apoptosis: the role of bacterial lipopolysaccharide. Sci Rep. 2020;10:9563.
18. Singh G, Guibao CD, Seetharaman J, Aggarwal A, Grace CR, McNamara DE, et al. Structural basis of BAK activation in mitochondrial apoptosis initiation. Nat Commun. 2022;13:250.
19. Zhang J, Niu H, Zhao ZJ, Fu X, Wang Y, Zhang X, et al. CRISPR/Cas9 Knockout of Bak Mediates Bax Translocation to Mitochondria in response to TNFα/CHX-induced Apoptosis. Biomed Res Int. 2019;2019:9071297.
20. Li C, Chen L, Song M, Fang Z, Zhang L, Coffie JW, et al. Ferulic acid protects cardiomyocytes from TNF-α/cycloheximide-induced apoptosis by regulating autophagy. Arch Pharm Res. 2020;43:863–74.
21. Gerlic M, Horowitz J, Horowitz S. Mycoplasma fermentans inhibits tumor necrosis factor alpha-induced apoptosis in the human myelomonocytic U937 cell line. Cell Death Differ. 2004;11:1204–12.
22. O'Donnell MA, Perez-Jimenez E, Oberst A, Ng A, Massoumi R, Xavier R, et al. Caspase 8 inhibits programmed necrosis by processing CYLD. Nat Cell Biol. 2011;13:1437–42.
23. Mai FY, He P, Ye JZ, Xu LH, Ouyang DY, Li CG, et al. Caspase-3-mediated GSDME activation contributes to cisplatin- and doxorubicin-induced secondary necrosis in mouse macrophages. Cell Prolif. 2019;52:e12663.
24. Taabazuing CY, Okondo MC, Bachovchin DA. Pyroptosis and apoptosis pathways engage in bidirectional crosstalk in monocytes and macrophages. Cell Chem Biol. 2017;24:507–14.e4.
25. Demarco B, Grayczyk JP, Bjanes E, Le Roy D, Tonnus W, Assenmacher CA, et al. Caspase-8-dependent gasdermin D cleavage promotes antimicrobial defense but confers susceptibility to TNF-induced lethality. Sci Adv. 2020;6:eabc3465.
26. Wang Y, Yin B, Li D, Wang G, Han X, Sun X. GSDME mediates caspase-3-dependent pyroptosis in gastric cancer. Biochem Biophys Res Commun. 2018;495:1418–25.
27. Rogers C, Fernandes-Alnemri T, Mayes L, Alnemri D, Cingolani G, Alnemri ES. Cleavage of DFNA5 by caspase-3 during apoptosis mediates progression to secondary necrotic/pyroptotic cell death. Nat Commun. 2017;8:14128.
28. Wang Y, Gao W, Shi X, Ding J, Liu W, He H, et al. Chemotherapy drugs induce pyroptosis through caspase-3 cleavage of a gasdermin. Nature. 2017;547:99–103.
29. Shi J, Zhao Y, Wang K, Shi X, Wang Y, Huang H, et al. Cleavage of GSDMD by inflammatory caspases determines pyroptotic cell death. Nature. 2015;526:660–5.
30. Ruan J. Structural insight of gasdermin family driving pyroptotic cell death. Adv Exp Med Biol. 2019;1172:189–205.
31. De Schutter E, Roelandt R, Riquet FB, Van Camp G, Wullaert A, Vandenabeele P. Punching holes in cellular membranes: biology and evolution of gasdermins. Trends Cell Biol. 2021;31:500–13.
32. Broz P, Pelegrín P, Shao F. The gasdermins, a protein family executing cell death and inflammation. Nat Rev Immunol. 2020;20:143–57.
33. Kayagaki N, Stowe IB, Lee BL, O'Rourke K, Anderson K, Warming S, et al. Caspase-11 cleaves gasdermin D for non-canonical inflammasome signalling. Nature. 2015;526:666–71.
34. Tang Y, Zhang R, Xue Q, Meng R, Wang X, Yang Y, et al. TRIF signaling is required for caspase-11-dependent immune responses and lethality in sepsis. Mol Med. 2018;24:66.
35. Yang D, He Y, Muñoz-Planillo R, Liu Q, Núñez G. Caspase-11 requires the pannexin-1 channel and the purinergic P2X7 pore to mediate pyroptosis and endotoxic shock. Immunity. 2015;43:923–32.
36. Nozaki K, Maltez VI, Rayamajhi M, Tubbs AL, Mitchell JE, Lacey CA, et al. Caspase-7 activates ASM to repair gasdermin and perforin pores. Nature. 2022;606:960–7.
37. Chen W, Qiang X, Wang Y, Zhu S, Li J, Babaev A, et al. Identification of tetranectin-targeting monoclonal antibodies to treat potentially lethal sepsis. Sci Transl Med. 2020;12:eaaz3833.
38. Saleh M, Mathison JC, Wolinski MK, Bensinger SJ, Fitzgerald P, Droin N, et al. Enhanced bacterial clearance and sepsis resistance in caspase-12-deficient mice. Nature. 2006;440:1064–8.
39. Seeley JJ, Baker RG, Mohamed G, Bruns T, Hayden MS, Deshmukh SD, et al. Induction of innate immune memory via microRNA targeting of chromatin remodelling factors. Nature. 2018;559:114–9.
40. Sha T, Sunamoto M, Kitazaki T, Sato J, Ii M, Iizawa Y. Therapeutic effects of TAK-242, a novel selective Toll-like receptor 4 signal transduction inhibitor, in mouse endotoxin shock model. Eur J Pharmacol. 2007;571:231–9.
41. Sheehan M, Wong HR, Hake PW, Malhotra V, O'Connor M, Zingarelli B. Parthenolide, an inhibitor of the nuclear factor-kappaB pathway, ameliorates cardiovascular derangement and outcome in endotoxic shock in rodents. Mol Pharmacol. 2002;61:953–63.
42. Wynn JL, Wilson CS, Hawiger J, Scumpia PO, Marshall AF, Liu JH, et al. Targeting IL-17A attenuates neonatal sepsis mortality induced by IL-18. Proc Natl Acad Sci USA. 2016;113:E2627–35.
43. Shakoory B, Carcillo JA, Chatham WW, Amdur RL, Zhao H, Dinarello CA, et al. Interleukin-1 receptor blockade is associated with reduced mortality in sepsis patients with features of macrophage activation syndrome: reanalysis of a prior phase III trial. Crit Care Med. 2016;44:275–81.
44. Vince JE, De Nardo D, Gao W, Vince AJ, Hall C, McArthur K, et al. The mitochondrial apoptotic effectors BAX/BAK activate caspase-3 and -7 to trigger NLRP3

inflammasome and caspase-8 driven IL-1beta activation. Cell Rep. 2018;25:2339–53.e4.
45. Walsh JG, Cullen SP, Sheridan C, Luthi AU, Gerner C, Martin SJ. Executioner caspase-3 and caspase-7 are functionally distinct proteases. Proc Natl Acad Sci USA. 2008;105:12815–9.
46. Gaidt MM, Ebert TS, Chauhan D, Schmidt T, Schmid-Burgk JL, Rapino F, et al. Human monocytes engage an alternative inflammasome pathway. Immunity. 2016;44:833–46.
47. Kang TB, Yang SH, Toth B, Kovalenko A, Wallach D. Caspase-8 blocks kinase RIPK3-mediated activation of the NLRP3 inflammasome. Immunity. 2013;38:27–40.
48. Fritsch M, Günther SD, Schwarzer R, Albert MC, Schorn F, Werthenbach JP, et al. Caspase-8 is the molecular switch for apoptosis, necroptosis and pyroptosis. Nature. 2019;575:683–7.
49. Zhang JY, Zhou B, Sun RY, Ai YL, Cheng K, Li FN, et al. The metabolite α-KG induces GSDMC-dependent pyroptosis through death receptor 6-activated caspase-8. Cell Res. 2021;31:980–97.
50. Sarhan J, Liu BC, Muendlein HI, Li P, Nilson R, Tang AY, et al. Caspase-8 induces cleavage of gasdermin D to elicit pyroptosis during Yersinia infection. Proc Natl Acad Sci USA. 2018;115:E10888–e97.
51. Chen KW, Demarco B, Heilig R, Shkarina K, Boettcher A, Farady CJ, et al. Extrinsic and intrinsic apoptosis activate pannexin-1 to drive NLRP3 inflammasome assembly. Embo J. 2019;38:e101638.
52. Wang Y, Karki R, Zheng M, Kancharana B, Lee S, Kesavardhana S, et al. Cutting edge: caspase-8 is a linchpin in caspase-3 and gasdermin D activation to control cell death, cytokine release, and host defense during influenza A virus infection. J Immunol. 2021;207:2411–6.
53. Rogers C, Erkes DA, Nardone A, Aplin AE, Fernandes-Alnemri T, Alnemri ES. Gasdermin pores permeabilize mitochondria to augment caspase-3 activation during apoptosis and inflammasome activation. Nat Commun. 2019;10:1689.
54. Pierini R, Juruj C, Perret M, Jones CL, Mangeot P, Weiss DS, et al. AIM2/ASC triggers caspase-8-dependent apoptosis in Francisella-infected caspase-1-deficient macrophages. Cell Death Differ. 2012;19:1709–21.
55. Van Opdenbosch N, Van Gorp H, Verdonckt M, Saavedra PHV, de Vasconcelos NM, Goncalves A, et al. Caspase-1 engagement and TLR-induced c-FLIP expression suppress ASC/Caspase-8-dependent apoptosis by inflammasome sensors NLRP1b and NLRC4. Cell Rep. 2017;21:3427–44.
56. Sagulenko V, Thygesen SJ, Sester DP, Idris A, Cridland JA, Vajjhala PR, et al. AIM2 and NLRP3 inflammasomes activate both apoptotic and pyroptotic death pathways via ASC. Cell Death Differ. 2013;20:1149–60.
57. Lamkanfi M, Kanneganti TD, Van Damme P, Vanden Berghe T, Vanoverberghe I, Vandekerckhove J, et al. Targeted peptidecentric proteomics reveals caspase-7 as a substrate of the caspase-1 inflammasomes. Mol Cell Proteomics. 2008;7:2350–63.
58. Kang SJ, Wang S, Hara H, Peterson EP, Namura S, Amin-Hanjani S, et al. Dual role of caspase-11 in mediating activation of caspase-1 and caspase-3 under pathological conditions. J Cell Biol. 2000;149:613–22.

ACKNOWLEDGEMENTS

We appreciated the carefully check of language by Dr. Chen, Jiong from Nanjing University. We also thank Prof. Shu Zhu from University of Science and Technology of China for providing the *Caspase11*-KO mice.

AUTHOR CONTRIBUTIONS

ZL and XG supervised the whole project. XL conceived, designed and performed experiments. XL, ZL, and XG analyzed the experiments and wrote the manuscript. TZ participated in the induction of necroptosis and Live-cell imaging experiments. RX and Qin Chen performed genotype identification of mice used in this project. LK, TZ, RX, Qianyue Chen and JP participated in the construction of septic mouse model. MS participated in the FACS experiments.

FUNDING

This work was supported by grants from the Ministry of Science and Technology of China (grant 2018YFA0801100 and 2021YFF0702100), the National Natural Science Foundation of China (grant 31971056, 31772550, 32000513), the Natural Science Foundation of Jiangsu Province (BK20181260), the Fundamental Research Funds for the Central Universities (14380516 and 021414380533).

COMPETING INTERESTS

The authors declare no competing interests.

ETHICS APPROVAL AND CONSENT TO PARTICIPATE

All mice were housed in a specific pathogen-free facility accredited by the Association for Assessment and Accreditation of Laboratory Animal Care International. All animal welfare and experimental procedures were approved by the Animal Care and Use Committee of the Model Animal Research Center, Nanjing University (Nanjing, China).

ADDITIONAL INFORMATION

Supplementary information The online version contains supplementary material available at https://doi.org/10.1038/s41418-023-01211-3.

Correspondence and requests for materials should be addressed to Xiang Gao or Zhaoyu Lin.

Reprints and permission information is available at http://www.nature.com/reprints

Publisher's note Springer Nature remains neutral with regard to jurisdictional claims in published maps and institutional affiliations.

Springer Nature or its licensor (e.g. a society or other partner) holds exclusive rights to this article under a publishing agreement with the author(s) or other rightsholder(s); author self-archiving of the accepted manuscript version of this article is solely governed by the terms of such publishing agreement and applicable law.